ARMA 14-7286

True triaxial tests in two porous sandstones: experimental failure characteristics and theoretical prediction

Ma, X.
Geological Engineering Program, University of Wisconsin-Madison, WI, USA (xma32@wisc.edu)
Rudnicki, J.W.
Department of Civil & Environmental Engineering and Department of Mechanical Engineering, Northwestern University, Evanston, IL, USA (jwrudn@northwestern.edu)
Haimson, B.C.
Department of Materials Science & Engineering, and Geological Engineering Program, University of Wisconsin-Madison, WI, USA (bhaimson@wisc.edu)

This paper was prepared for presentation at the 48th US Rock Mechanics / Geomechanics Symposium held in Minneapolis, MN, USA, 1-4 June 2014.

ABSTRACT: True triaxial tests have been carried out in two quartz-rich, high porosity, sandstones, Coconino (n = 17.5%) and Bentheim (n = 24%) by maintaining constant but different σ_2 and σ_3 and raising σ_1 until failure occurred (at $\sigma_{1,peak}$). For each constant σ_3 level, σ_2 was varied from test to test between $\sigma_2 = \sigma_3$ and $\sigma_2 = \sigma_1$. $\sigma_{1,peak}$ for a given σ_3 increased with σ_2, reached a maximum (up to 15% higher than when $\sigma_2 = \sigma_3$), and then declined so that when σ_2 approached σ_1, $\sigma_{1,peak}$ was about equal to its base value when $\sigma_2 = \sigma_3$. A separate series of tests was carried out using a novel loading path by maintaining constant Lode angle Θ (= 0°). This series of tests characterized the dependence of the octahedral shear stress at failure $\tau_{oct,f}$ on the octahedral normal stress at failure $\sigma_{oct,f}$ when Θ = 0°. The latter tests were used to obtain the necessary parameters employed in a three-invariant failure theory proposed by *Rudnicki* (2013). The theory was then applied to predicting the variation of $\sigma_{1,peak}$ with σ_2 for a given σ_3. The prediction reasonably replicated the typical ascending-then-descending $\sigma_{1,peak}$ vs. σ_2 trend observed experimentally in both sandstones, confirming (with some limitations) the applicability of the *Rudnicki*'s (2013) theory.

1. INTRODUCTION

The failure of rocks subjected to a general state of stress ($\sigma_1 \geq \sigma_2 \geq \sigma_3$) has been studied since the pioneering true triaxial experiments conducted by *Mogi* [1]. In true triaxial tests, cuboidal specimens are subjected to fixed, and typically unequal, σ_3 and σ_2, while σ_1 is increased until failure occurs (expressed by σ_1 at failure, or $\sigma_{1,peak}$). For each constant σ_3, σ_2 is varied from test to test between $\sigma_2 = \sigma_3$ and σ_2 approaching σ_1. The important effect of the intermediate principal stress (σ_2) on $\sigma_{1,peak}$ has been demonstrated in a number of rocks [1-6]. As σ_2 is raised above the fixed σ_3, $\sigma_{1,peak}$ first rises, but reaches a plateau at an intermediate σ_2 level, beyond which it gradually declines. The variation of $\sigma_{1,peak}$ with σ_2 contradicts the *Mohr-Coulomb* failure criterion, which neglects the role of σ_2 in the failure process.

The University of Wisconsin true triaxial testing apparatus has been used for studying failure characteristics of several crystalline and clastic rocks subjected to a general state of stress ($\sigma_1 \geq \sigma_2 \geq \sigma_3$) [2-6]. All rocks except for Long Valley Caldera hornfels and metapelite [4] exhibited consistent σ_2 effect on failure. In the study presented here, we tested two porous, quartz-rich sandstones, Coconino and Bentheim, with significantly higher porosities than those used in previous true triaxial tests. The motivation for this study was two-fold: (1) study the effect of σ_2 on rock failure, and (2) examine the applicability of a theory to failure prediction.

2. PHYSICAL AND MECHANICAL PROPERTIES OF TESTED SANDSTONES

The two porous sandstones tested in this study, Coconino and Bentheim, are both quartz-rich (> 90%), but differ considerably in porosity, grain size, and strength (Table 1). Coconino sandstone is an early Permian aeolian sedimentary rock with medium-to-high porosity (n = 17.5%). Bentheim sandstone is a Lower Cretaceous sedimentary rock from Bentheim, Germany. It has a much higher porosity (n = 24%).

Though both rocks are bedded sandstones, their uniaxial deformational and strength characteristics in and perpendicular to the bedding planes show only marginal discrepancies (Table 1). Hence, it was concluded that

Table 1. Summary of some physical and mechanical properties of both sandstones

Property	Coconino	Bentheim
Mineral composition	99% quartz <1% iron oxide	95% quartz 3% feldspar 2% kaolinite
Primary grain bonding	Qtz overgrowth sutures	Qtz sutured
Mean grain size (mm)	0.1 ± 0.03	0.3 ± 0.03
Sorting	Well sorted	Well sorted
Grain geometry	Rounded	sub-rounded
Effective porosity (%)	17.5 ± 0.4 (10)*	24.0 ± 0.8 (10)
Density (g/cm^3)	2.23 ± 0.01 (10)	2.00 ± 0.01 (10)
UCS (MPa)	56.1 ± 5.1 (10)	30.0 ± 3.4 (10)
Young's modulus, *E* (GPa)	28 ± 4.6 (10)	10.5 ± 0.8 (10)
Poisson's ratio, *v*	0.25 ± 0.05 (10)	0.36 ± 0.05 (10)

* Number in parentheses indicates the amount of tests run.

both sandstones can be construed as practically isotropic for the purpose of the present research. For consistency purposes, all specimens tested were prepared from a single block and cut so that their long axis was perpendicular to bedding.

3. EXPERIMENTAL SETUP AND PROCEDURE

Experiments were conducted using our true triaxial testing assembly (for details, see [2]). A square cuboidal specimen (19×19×38 mm^3) is inserted into the cell and independently compressed along three principal directions. The maximum and intermediate principal stresses, σ_1 and σ_2, are transmitted through two pairs of hydraulically driven pistons activated in the biaxial apparatus. The minimum principal stress σ_3 is applied directly by the confining fluid injected into the cell. A thin layer of polyurethane painted on the pair of specimen faces subjected to σ_3 prevents the fluid from contacting the rock.

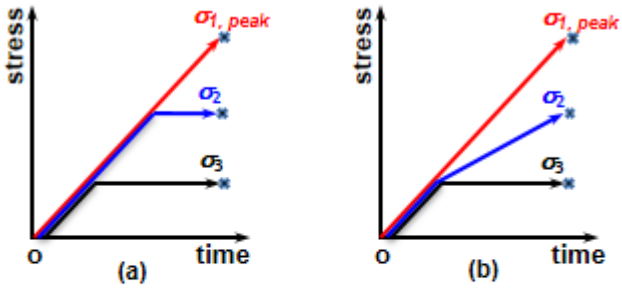

Fig. 1. Two methods of true triaxial tesing: (a) common loading path (σ_2 and σ_3 constant, σ_1 increasing monotonically), and (b) novel loading path (σ_3 constant, σ_2 and σ_1 rising while maintaining constant $(\sigma_2 - \sigma_3)/(\sigma_1 - \sigma_3)$ ratio).

A series of true triaxial tests was performed using the common loading path (Figure 1a), similar to that in previous true triaxial experiments [1-6], that is, maintaining σ_2 and σ_3 at preset magnitudes while raising σ_1 monotonically at a rate of 0.1 MPa/s until failure occurred ($\sigma_{1,peak}$ was reached). For each constant level of σ_3, tests were conducted between $\sigma_2 = \sigma_3$ and $\sigma_1 = \sigma_2$.

A separate series of true triaxial tests was performed using a novel loading path, σ_3 was kept constant while σ_1 and σ_2 were raised at a fixed ratio b [$= (\sigma_2 - \sigma_3)/(\sigma_1 - \sigma_3)$] until failure occurred (Figure 1b). The loading rate for σ_1 was kept at a constant 0.1 MPa/s. The constant stress ratio b maintained a fixed Lode angle Θ [7]:

$$\Theta = \tan^{-1}\left(\frac{1-2b}{\sqrt{3}}\right) \quad (1)$$

Specifically, this novel loading path was used to characterize the dependence of failure (in the form of $\tau_{oct,f}$) on $\sigma_{oct,f}$ when $\Theta = 0°$ ($b = 1/2$).

4. EXPERIMENTAL RESULTS

The variation of $\sigma_{1,peak}$ with σ_2 for each of the σ_3 magnitudes applied is shown in Figure 2. In both rocks, $\sigma_{1,peak}$ increased with σ_2, until a maximum was reached, beyond which the failure point gradually declined, so that when σ_2 approached σ_1, $\sigma_{1,peak}$ was approximately equal to its base value when $\sigma_2 = \sigma_3$. The typical ascending-then-descending $\sigma_{1,peak}$ vs. σ_2 trend could be well expressed by a polynomial curve of the second order (Figure 2). The solid curve in Figure 2, fitted to test data for which $\sigma_2 = \sigma_3$, represents the *Mohr* failure criterion ($\sigma_{1,peak} = f(\sigma_3)$). A dotted line fits the data points for triaxial extension ($\sigma_2 = \sigma_1$). Figure 2 demonstrates that $\sigma_{1,peak}$ is a function of not only σ_3, but also of σ_2, as observed previously in other rock types [1-6]. Generally, the maximum $\sigma_{1,peak}$ for a constant σ_3 in both sandstones is no more than 15% higher than $\sigma_{1,peak}$ when $\sigma_2 = \sigma_3$, and this rise in $\sigma_{1,peak}$ with σ_2 is appreciably less pronounced than in previously tested low-porosity rocks [1,2,3,5,6].

All failure related experimental results can be represented by a single relationship in terms of two principal stress invariants, octahedral shear stress at failure ($\tau_{oct,f}$) and octahedral normal stress at failure ($\sigma_{oct,f}$):

$$\tau_{oct,f} = f\left(\sigma_{oct,f}\right) \quad (2)$$

As shown in Figure 3, $\tau_{oct,f}$ rose with $\sigma_{oct,f}$, albeit at a decreasing rate. The best fitting curve representing $\tau_{oct,f}$ as a function of $\sigma_{oct,f}$ in both sandstones is a polynomial of the second order (Figure 3). In Coconino sandstone, $\tau_{oct,f}$ at the highest applied $\sigma_{oct,f}$ (= 460 MPa), was still

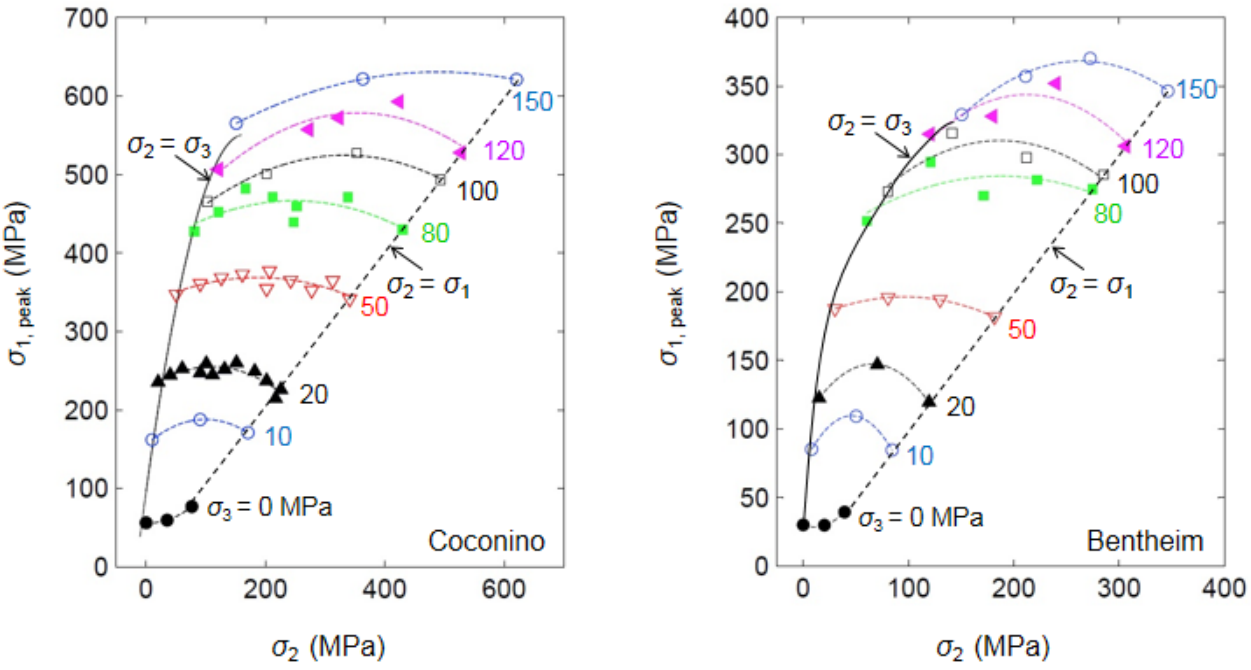

Fig. 2. Variation of $\sigma_{1,peak}$ with σ_2 in Coconino and Bentheim sandstones tested under true triaxial stresses for all constant σ_3 levels: the solid curve represents the *Mohr* failure criterion when $\sigma_2 = \sigma_3$ and the dashed straight line connects data points of $\sigma_2 = \sigma_1$.

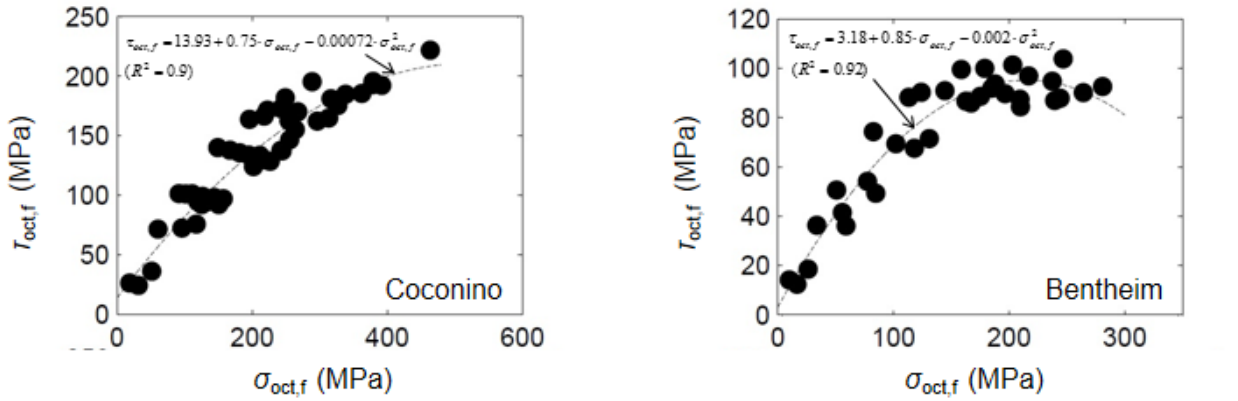

Fig. 3. Variation of the octahedral shear stress at failure ($\tau_{oct,f}$) with the octahedral normal stress at failure ($\sigma_{oct,f}$) in Coconino and Bentheim sandstones subjected to true triaxial stresses. All data points were correlated with a second-order polynomial equation.

rising even if at a very reduced rate. In Bentheim sandstone, however, $\tau_{oct,f}$ gradually leveled off at $\sigma_{oct,f}$ = 150 MPa and began to decline for larger $\sigma_{oct,f}$, forming a 'cap'. The cap is often found in weak, porous rocks subjected to high compressive stresses. The cap is the result of partial pore collapse and grain crushing due to high normal stress $\sigma_{oct,f}$ [8].

The results of true triaxial tests using a novel loading path, in which the Lode angle Θ (= 0°) was maintained constant during testing, are also shown in the $\tau_{oct,f}$ - $\sigma_{oct,f}$ domain (Figure 4). The variation of $\tau_{oct,f}$ with $\sigma_{oct,f}$ at Θ = 0°, resembles the general trend shown by tests conducted under constant σ_2 and σ_3 in Figure 3. Experimental results of tests conducted at Θ = 0°, shown in Figure 4, can be well-fitted by a second-order polynomial equation, which holds true for the specific case of Θ = 0°:

for Coconino,

$$\tau_{oct,f0}\left(\equiv \tau_{oct,f}\big|_{\Theta=0}\right) = 8.377 + 0.697 \cdot \sigma_{oct,f} - 0.00054 \cdot \sigma^2_{oct,f} \quad (3)$$

for Bentheim,

$$\tau_{oct,f0}\left(\equiv \tau_{oct,f}\big|_{\Theta=0}\right) = -1.445 + 0.833 \cdot \sigma_{oct,f} - 0.002 \cdot \sigma^2_{oct,f} \quad (4)$$

5. COMPARISON OF FAILURE WITH A THEORY

An attempt was made to compare experimental failure results with a three-invariant failure theory. An expression proposed by *Rudnicki* [7] was employed:

$$F\left(\tau_{oct,f},\sigma_{oct,f},\Theta\right) = -\sqrt{\frac{4}{27}}\cdot A\cdot\sin\left(3\Theta\right)\cdot\left(\frac{\tau_{oct,f}}{\tau_{oct,f0}}\right)^3+\left(\frac{\tau_{oct,f}}{\tau_{oct,f0}}\right)^2-1=0 \quad (5)$$

where A is a measure of the discrepancy between the magnitude of $\tau_{oct,f}$ in axisymmetric compression and that in axisymmetric extension for the same level of $\sigma_{oct,f}$. This discrepancy, if any, represents the dependence of $\tau_{oct,f}$ on Lode angle Θ. Valid magnitudes of A are limited to between -1 and +1 [7]. Both $\tau_{oct,f0}$ and A are functions of $\sigma_{oct,f}$. When Θ = 0°, the first term of Eq. (5) vanishes and the equation is reduced to $\tau_{oct,f}|_{\Theta=0} = \tau_{oct,f0}$ ($\sigma_{oct,f}$), so that $\tau_{oct,f0}$ represents the dependence of $\tau_{oct,f}$ on $\sigma_{oct,f}$ under the deviatoric pure shear stress state (Θ = 0°). Similarly, When A = 0, the first term in Eq. (5) vanishes, and the equation is reduced to $\tau_{oct,f} = \tau_{oct,f0}$ ($\sigma_{oct,f}$), implying no failure ($\tau_{oct,f}$) variation with Θ.

The specific form of $\tau_{oct,f} = \tau_{oct,f0}$ ($\sigma_{oct,f}$) is derived from the experimental results of variation of $\tau_{oct,f}$ versus $\sigma_{oct,f}$ under pure shear (Θ = 0°) (Equations 3 and 4). Data from the constant σ_2 and σ_3 tests are used to infer the dependence of A on $\sigma_{oct,f}$ using Equations 3 and 4. For each set of $\sigma_{1,peak}$, σ_2 and σ_3, the set of invariants $\tau_{oct,f}$, $\sigma_{oct,f}$ and Θ were calculated. These were used with $\tau_{oct,f0}$ ($\sigma_{oct,f}$) to calculate values of A from Eq. (5). The corresponding values of A are shown in Figure 5. A is clearly a monotonically decreasing function of $\sigma_{oct,f}$, i.e., $A = A$ ($\sigma_{oct,f}$), and the specific expression of A is empirically determined. A linear equation is found to describe the variation of A with $\sigma_{oct,f}$ well (Figure 5):

for Coconino,

$$A(\sigma_{oct,f}) = 1.019 - 0.002\cdot\sigma_{oct,f} \quad (6)$$

for Bentheim,

$$A(\sigma_{oct,f}) = 1.245 - 0.006\cdot\sigma_{oct,f} \quad (7)$$

The scatter of the results for A suggests that the form of Eq. (5) does not precisely capture the variation of $\tau_{oct,f}$ with Θ for constant $\sigma_{oct,f}$.

The linear form for A, Eq. (6) and Eq. (7), and the quadratic forms for $\tau_{oct,f0}$, Eq. (3) and Eq. (4), are substituted into Eq. (5), to predict the variation of $\sigma_{1,peak}$ with σ_2 for each constant σ_3.

The variation of $\sigma_{1,peak}{}^T$ (superscript 'T' denoting theoretical prediction) with σ_2 for each constant σ_3 is calculated by increasing the variable σ_2 in infinitesimal increments from its lower limit (= σ_3) to the upper limit (= σ_1). The predicted continuous $\sigma_{1,peak}{}^T$ along with the experimental data points ($\sigma_{1,peak}$) are compared in Figure 6. The failure predictions in both Coconino and

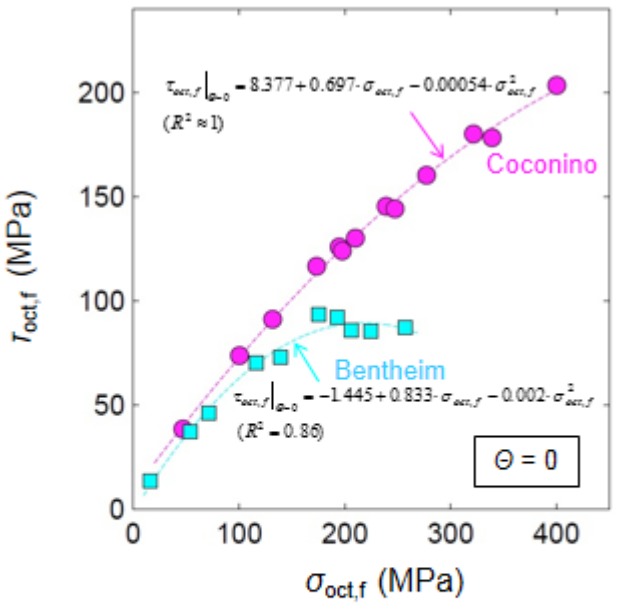

Fig. 4. Variation of the octahedral shear stress at failure ($\tau_{oct,f}$) with the octahedral normal stress at failure ($\sigma_{oct,f}$) in Coconino and Bentheim sandstones tested using the constant Θ (= 0) loading path: the data points were fitted with a second-order polynomial equation.

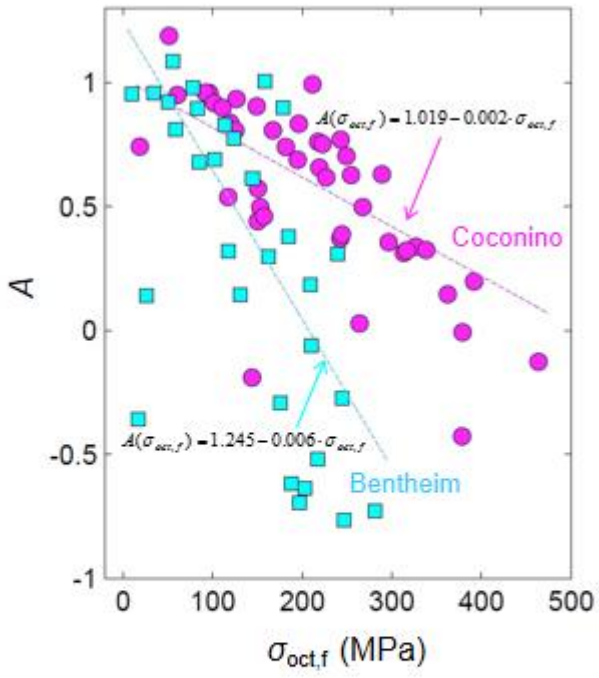

Fig. 5. Variation of A with the octahedral normal stress at failure ($\sigma_{oct,f}$) in Coconino and Bentheim sandstones in true triaxial tests: the dashed line represents the best linear regression of all data points in each rock.

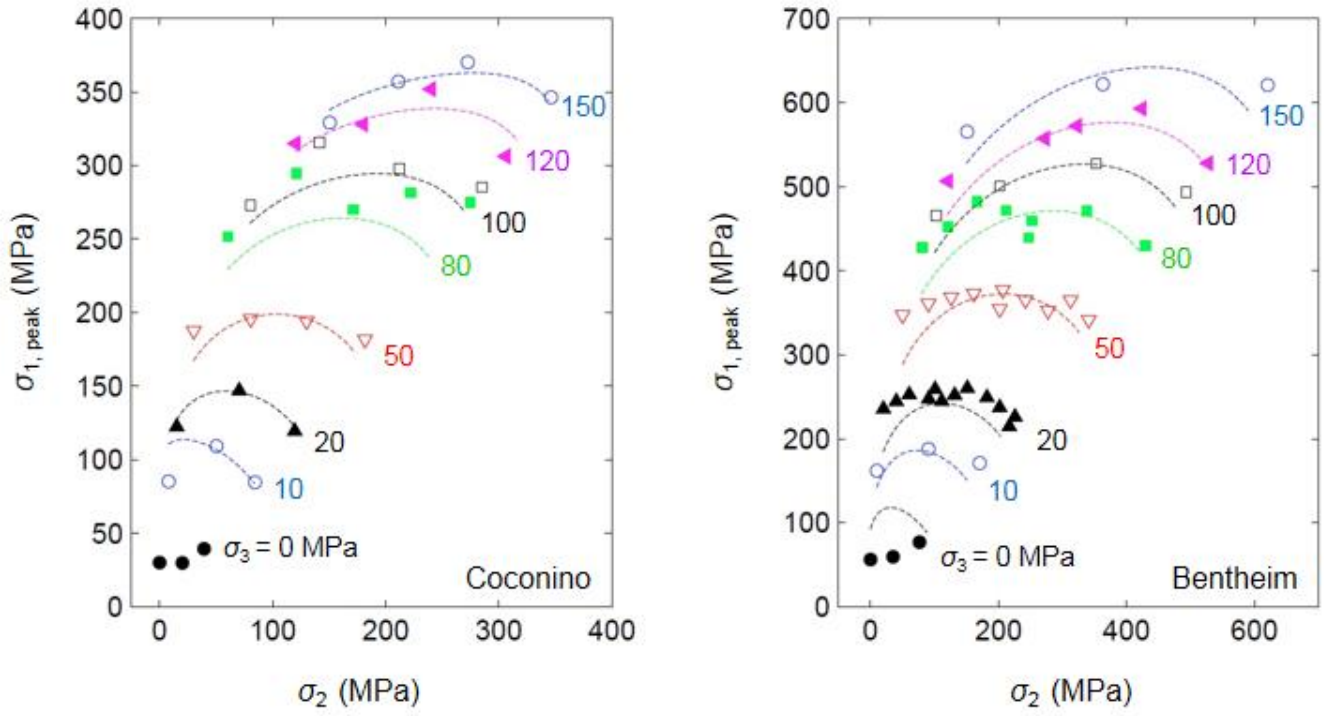

Fig. 6. Variation of $\sigma_{1,peak}$ with σ_2 in the true triaxial (constant σ_2 and σ_3), experimental data (symbols) and predicted conditions (dashed lines) for all constant σ_3 series, in Coconino and Bentheim sandstones.

Bentheim sandstones generally replicate the variation of $\sigma_{1,peak}$ with σ_2 observed experimentally. The increase of σ_2 first brings about the rise in $\sigma_{1,peak}{}^T$, which reaches its maximum at an intermediate level of σ_2, then consistently declines for larger σ_2, comparable to experimental results. However, $\sigma_{1,peak}{}^T$ at both $\sigma_2 = \sigma_3$ and $\sigma_2 = \sigma_1$ are lower than the experimentally obtained magnitudes by about 10%. The prediction in general produces a higher $\sigma_{1,peak}{}^T$ at $\sigma_2 = \sigma_1$ than at $\sigma_2 = \sigma_3$. The theoretical prediction did not return reasonable values at σ_3 = 0 MPa in both sandstones. This was caused by the excessive magnitude of A at σ_3 = 0 MPa (larger than +1, the maximum permitted value by Eq. (5).

6. CONCLUSIONS

In both Coconino and Bentheim sandstones, failure in the form of $\sigma_{1,peak}$ for a constant σ_3 rose as σ_2 was elevated above σ_3 from test to test. At some point between σ_3 and σ_1, $\sigma_{1,peak}$ reached a maximum, then monotonically declined for larger σ_2. The maximum $\sigma_{1,peak}$ for a given σ_3 was limited to less than 15% increase beyond $\sigma_{1,peak}$ at $\sigma_2 = \sigma_3$, significantly less than that observed in low-porosity crystalline and clastic rocks. The typical ascending-then-descending $\sigma_{1,peak}$ vs. σ_2 trend for a constant σ_3 reveals the limitations of the conventional triaxial testing ($\sigma_2 = \sigma_3$), in which the σ_2 effect is not considered.

The stress conditions at failure in both sandstones can be represented by a single relationship in terms of $\tau_{oct,f}$ and $\sigma_{oct,f}$, fitted by a second-order polynomial equation. The average $\tau_{oct,f}$ initially rises with $\sigma_{oct,f}$, but at a decreasing rate. Over the same range of the applied σ_3 (between 0 and 150 MPa), the rate of $\tau_{oct,f}$ increase with $\sigma_{oct,f}$ in Bentheim sandstone dropped much faster than in Coconino so that its average $\tau_{oct,f}$ eventually reached a 'cap' beyond which it appeared to decline for larger $\sigma_{oct,f}$. This suggests that the more porous and weaker Bentheim begins the process of localized compaction (failure) at a lower stress condition than the Coconino.

Rudnicki [7] presents a failure theory in terms of three principal stress invariants. Comparison of failure ($\sigma_{1,peak}$) between prediction based on this theory and experimental data generally confirms its applicability to representing the stress conditions at failure in both sandstones when subjected to true triaxial loading.

ACKNOWLEDGEMENT

This research is supported by the National Science Foundation Grant EAR-0940323.

REFERENCES

1. Mogi, K. 1971. Fracture and flow of rocks under high triaxial compression, *J. Geophys. Res.* 76: 1255-1269.

2. Haimson, B. and C. Chang. 2000. A new true triaxial cell for testing mechanical properties of rock, and its use to determine rock strength and deformability of Westerly granite. *Int. J. Rock Mech. & Min. Sci.* 37: 285-296.

3. Chang, C. and B. Haimson. 2000. True triaxial strength and deformability of the German Continental Deep Drilling Program (KTB) deep hole amphibolite. *J. Geophys. Res.* 105: 18,999-19,013.

4. Chang, C. and B. Haimson. 2005. Non-dilatant deformation and failure mechanism in two Long Valley Caldera rocks under true triaxial compression. True triaxial strength and deformability of the German Continental Deep Drilling Program (KTB) deep hole amphibolite. *Int. J. Rock Mech. & Min. Sci.* 42: 402-414.

5. Oku, H., B. Haimson, and S.R. Song. 2007. True triaxial strength and deformability of the siltstone overlying the Chelungpu fault (Chi-Chi earthquake), Taiwan. *Geophys. Res. Lett.* 34: L90306.

6. Lee, H. and B. Haimson. 2011. True triaxial strength, deformability, and brittle failure of granodiorite from the San Andreas Fault Observatory at depth. *Int. J. Rock Mech. & Min. Sci.* 48: 1199-1207.

7. Rudnicki, J. W. 2013. Failure of Rocks in the Laboratory and in the Earth, in *Proceedings of 22nd International Congress on Theoretical and Applied Mechanics Adelaide, Australia 24 – 29 August, 2008*, eds. J. P. Denier and M. D. Finn, pp. 199-215, Springer.

8. Olsson, W. A. 1999. Theoretical and experimental investigation of compaction bands in porous rock, *J. Geophys. Res.* 104: 7219–7228